Chapter 3
Select Equations to Be Solved

3.1 Fluid Mechanics Analysis System: Reynolds Transport Theorem

Fluid mechanics mainly applies three conservation laws of mass, energy, and momentum to the fluid flow (called governing equations of flow) and predicts the flow characteristics and the interactions among fluids as well as with solids. The mass, momentum, and energy conservation laws can be applied using two different analysis systems—closed system and open system.

(1) **Closed system (fixed mass or control mass system): Lagrangian System**

In a closed system, objects with fixed mass (e.g., a solid ball) are isolated and their changes in energy and momentum are tracked along with relevant properties such as pressure, velocity, temperature, etc (Fig. 3.1). The size and shape of the system may change during a process but there is no mass transfer in or out through the boundaries of this control mass. Closed systems are mostly used in thermodynamics and solid mechanics, where the state and movement of a certain object are the focus. For fluid mechanics, most cases are interested in the flow characteristics contained in a confined space rather than the pre- and post-fates of fluid before entering and after leaving the container. For instance, in indoor environment quality study, one may concentrate on the temperature and velocity distributions in a room caused by supply and exhaust diffusers, while ignoring where the air comes from and exhausts to. On the other hand, tracking the boundaries and movement of a fluid mass is much more challenging than tracking a solid mass due to irregularity and sometimes discontinuity of fluid geometry (such as when splattering). Nevertheless, a closed system may be used for some fluid flow problems such as tracking the trajectories of virus transportation in a space, where the specific objects (virus in this case) are the focused interest of the study.

(2) **Open system (fixed volume or control volume system): Euler System**

In an open system, the volume of a space is isolated and studied for the changes of mass, energy, and momentum in this volume during a process. The system allows the

Z. Zhai, *Computational Fluid Dynamics for Built and Natural Environments*, https://doi.org/10.1007/978-981-32-9820-0_3

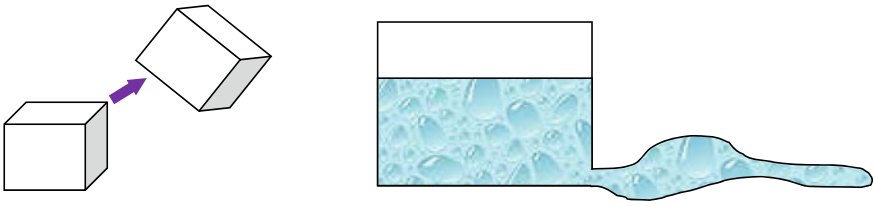

Fig. 3.1 Illustrations of using closed system for solid (left) and fluid (right)

flow in and out of mass, energy and momentum across the boundaries (called control surfaces) of the control volume. A control volume may also move and deform during a process, although most real-world applications utilize fixed and non-deformable control volumes to simplify the problems in study.

Another analogy to distinguish the control mass from the control volume system is to monitor students in a classroom. If the goal is to track the movement and properties of every student during the whole process (even before and after the class), one needs to track individual students (fixed mass) before they enter or after they leave the classroom. This is a closed system analysis. If the goal is to simply count student number in the classroom (without interest in where they come from and leave for), the classroom is the fixed or control volume to be explored and thus an open system should be used to allow students enter and leave the room.

(3) **Conversion from closed system to open system with Reynolds Transport Theorem**

Although different systems can be used to analyze the status of objects, the physics in conservation laws is uniform and independent of the analysis system selected. The Reynolds transport theorem (RTT) provides the link between the control mass and the control volume approaches, converting the conservation equations in one system to the other. The following provides the general format of the RTT:

$$\frac{dB_{CM}}{dt} = \frac{dB_{CV}}{dt} - \dot{B}_{in} + \dot{B}_{out} \tag{3.1}$$

where B can be any variable (such as mass, energy, and momentum). CM stands for control mass and CV stands for control volume. $\dot{B}$ is the flow rate of variable in and out of the control volume.

3.2 Fluid Mechanics Conservation Equations in Integral Form

(1) **Mass Conservation**

If B = M (mass), Eq. (3.1) becomes

$$\frac{dM_{CM}}{dt} = \frac{dM_{CV}}{dt} - \dot{M}_{in} + \dot{M}_{out} \tag{3.2}$$

Since for a control mass, M does not change with time,

$$\frac{dM_{CM}}{dt} = 0 = \frac{dM_{CV}}{dt} - \dot{M}_{in} + \dot{M}_{out} \tag{3.3}$$

The mass conservation equation for a control volume is thus

$$\frac{dM_{CV}}{dt} = \dot{M}_{in} - \dot{M}_{out} \tag{3.4}$$

The mass change in a control volume is attributed to the imbalance between the mass flow in and the mass flow out. For a steady flow, d/dt = 0 for any variable,

$$\dot{M}_{in} = \dot{M}_{out} \tag{3.5}$$

This $\dot{M}$ may imply the sum of multiple inlets and outlets to the control volume.

(2) **Energy Conservation**

If B = E (total energy), Eq. (3.1) becomes

$$\frac{dE_{CM}}{dt} = \frac{dE_{CV}}{dt} - \dot{E}_{in} + \dot{E}_{out} \tag{3.6}$$

where E is the total energy (including both mechanical and thermal energy); $E = H + E_P + E_K = U + PV + E_P + E_K$. $H = U + PV = mC_PT$ is enthalpy; $U = mC_VT$ is internal energy. C_P and C_V are specific heat at constant pressure and constant volume, respectively. T is temperature, P is pressure and V is volume. $E_P = mgz$ is potential energy, and $E_k = mv^2/2$ is kinetic energy (v is velocity). $\dot{E}$ is the flow rate of total energy in and out of the control volume.

The first law of thermodynamics states

$$\frac{dE_{CM}}{dt} = \dot{Q} + \dot{W} + \dot{S} \tag{3.7}$$

where $\dot{Q}$ is the heat transfer (rate) imposed on the volume, $\dot{W}$ is the mechanical work (rate) conducted on the volume, and $\dot{S}$ is any additional energy (rate) occurred during the process (such as from chemical or nuclear reactions etc.). Hence, for a control volume (Fig. 3.2),

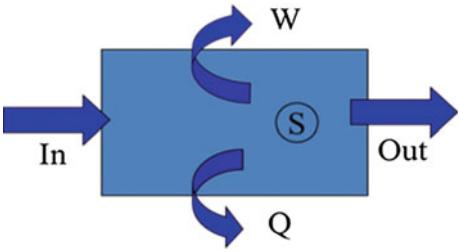

Fig. 3.2 Illustration of energy conservation in a control volume

$$\frac{dE_{CV}}{dt} = \dot{E}_{in} - \dot{E}_{out} + \dot{Q} + \dot{W} + \dot{S} \tag{3.8}$$

(3) **Momentum Conservation**

If $B = M\vec{V}$(momentum), Eq. (3.1) provides

$$\frac{d(M\vec{V})_{CM}}{dt} = \frac{d(M\vec{V})_{CV}}{dt} - (\dot{M}\vec{V})_{in} + (\dot{M}\vec{V})_{out} \tag{3.9}$$

where $\vec{V}$ is the velocity vector, and $\dot{M}$ is the mass flow rate at inlet and outlet.

The Newton's second law for a control mass states:

$$\frac{d(M\vec{V})_{CM}}{dt} = \sum \vec{F} \tag{3.10}$$

where the force $\vec{F}$ includes various body and surface forces such as gravity (body), pressure (normal stress at surfaces), and friction (shear stress at surfaces) forces. Combining Eqs. (3.9) and (3.10) yields

$$\frac{d(M\vec{V})_{CV}}{dt} - (\dot{M}\vec{V})_{in} + (M\vec{V})_{out} = \sum \vec{F} \tag{3.11}$$

For a steady flow,

$$(\dot{M}\vec{V})_{out} - (\dot{M}\vec{V})_{in} = \sum \vec{F} \tag{3.12}$$

Again, $\dot{M}\vec{V}$ here implies the summary of momentum forces at various inlets and outlets of the control volume in study.

3.3 Fluid Mechanics Conservation Equations in Differential Form

The section above presents the fundamental flow governing equations in the integral form, which clearly reveals the principles of the conservation of mass, energy and momentum in fluid flow in a control volume. The integral expression of the governing equation is good for manual calculation for simplified flow problems, such as with steady, one-dimensional assumptions, and for computing average flow properties (e.g., one single temperature and velocity for the entire volume). To predict complex fluid flows with adequate spatial and temporal resolutions using a computer, the differential form of flow governing equations must be introduced and used.

To ease the writing and reading of a lengthy mathematic equation, the Einstein notation is often used in mathematics. The Einstein notation or Einstein summation convention is a notational convention that implies summation over a set of indexed terms in a formula, thus achieving notational brevity. It was introduced by Albert Einstein in 1916. According to this convention, when an index variable appears twice in a single term it implies summation of that term over all the values of the index (e.g., 1, 2, and 3 for a 3-D problem while 1 and 2 for a 2-D problem). Below are a few examples that are commonly seen in fluid mechanics:

- $\mathrm{U_i U_i} = \mathrm{U_1 U_1} + \mathrm{U_2 U_2} + \mathrm{U_3 U_3}$ ($\mathrm{U_1} = \mathrm{U}$, $\mathrm{U_2} = \mathrm{V}$, $\mathrm{U_3} = \mathrm{W}$ in a 3-D flow)
- $\frac{dU_i}{dx_i} = \frac{dU_1}{dx_1} + \frac{dU_2}{dx_2} + \frac{dU_3}{dx_3}$ ($\mathrm{x_1} = \mathrm{x}$, $\mathrm{x_2} = \mathrm{y}$, $\mathrm{x_3} = \mathrm{z}$ in a 3-D flow)
- $U_j \frac{dU_i}{dx_j} = U_1 \frac{dU_i}{dx_1} + U_2 \frac{dU_i}{dx_2} + U_3 \frac{dU_i}{dx_3}$ (where i can be any one but only one of 1, 2, 3)
- $\frac{\partial^2 \tau_{ij}}{\partial x_i \partial x_j} = \frac{\partial^2 \tau_{11}}{\partial x_1 \partial x_1} + \frac{\partial^2 \tau_{12}}{\partial x_1 \partial x_2} + \frac{\partial^2 \tau_{13}}{\partial x_1 \partial x_3} + \frac{\partial^2 \tau_{21}}{\partial x_2 \partial x_1} + \frac{\partial^2 \tau_{22}}{\partial x_2 \partial x_2} + \frac{\partial^2 \tau_{23}}{\partial x_2 \partial x_3} + \frac{\partial^2 \tau_{31}}{\partial x_3 \partial x_1} + \frac{\partial^2 \tau_{32}}{\partial x_3 \partial x_2} + \frac{\partial^2 \tau_{33}}{\partial x_3 \partial x_3}$
  (Here one pair of i and one pair of j appear and thus each of i and j should expand over all the values of the index).

For a single-phase Newtonian fluid (where viscosity does not depend on flow velocity and stress state), the general governing equations of flow may be expressed as below, in a Cartesian coordinate system.

(1) **Continuity Equation (Mass Conservation)**

$$\frac{\partial \rho}{\partial \mathrm{t}} + \frac{\partial}{\partial x_\mathrm{j}}\left(\rho \mathrm{u_j}\right) = 0 \tag{3.13}$$

where, ρ is the air density, $\mathrm{u_j}$ is the instantaneous velocity component in three perpendicular coordinate directions ($\mathrm{x_j}$, $\mathrm{j} = 1, 2, 3$), and t is the time.

The following presents the derivation of the continuity equation. For an infinite small volume (or cell/mesh) dv, the cell center holds the velocity u, v, w at the coordinate of (x, y, z). The mass flow rate at the surface of ($\mathrm{x} - 0.5\mathrm{dx}$) (called west surface) into the cell is thus:

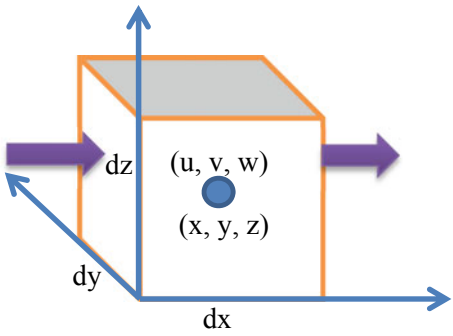

Fig. 3.3 Illustration of mass conservation over a control volume dv = dxdydz

$$\dot{m}_{x-0.5dx} = \left[\rho u - \frac{\partial}{\partial x}(\rho u) \cdot \frac{1}{2}dx\right] \cdot dydz \tag{3.14}$$

And the mass flow rate at the surface of (x + 0.5dx) (called east surface) out of the cell is:

$$\dot{m}_{x+0.5dx} = \left[\rho u + \frac{\partial}{\partial x}(\rho u) \cdot \frac{1}{2}dx\right] \cdot dydz \tag{3.15}$$

dydz is the area of west and east surfaces as illustrated in Fig. 3.3. The net mass flow rate on the X coordinate is then:

$$\begin{aligned}
&\dot{m}_{x-0.5dx} - \dot{m}_{x+0.5dx} \\
&= \left[\rho u - \frac{\partial}{\partial x}(\rho u) \cdot \frac{1}{2}dx\right] \cdot dydz - \left[\rho u + \frac{\partial}{\partial x}(\rho u) \cdot \frac{1}{2}dx\right] \cdot dydz \\
&= -\frac{\partial}{\partial x}(\rho u) \cdot dxdydz
\end{aligned} \tag{3.16}$$

Similarly, the net mass flow rate on the Y and Z coordinates can be obtained, respectively:

$$\begin{aligned}
&\dot{m}_{y-0.5dy} - \dot{m}_{y+0.5dy} \\
&= \left[\rho v - \frac{\partial}{\partial y}(\rho v) \cdot \frac{1}{2}dy\right] \cdot dxdz - \left[\rho v + \frac{\partial}{\partial y}(\rho v) \cdot \frac{1}{2}dy\right] \cdot dxdz \\
&= -\frac{\partial}{\partial y}(\rho v) \cdot dxdydz
\end{aligned} \tag{3.17}$$

$$\begin{aligned}
&\dot{m}_{z-0.5dz} - \dot{m}_{z+0.5dz} \\
&= \left[\rho w - \frac{\partial}{\partial z}(\rho w) \cdot \frac{1}{2}dz\right] \cdot dxdy - \left[\rho w + \frac{\partial}{\partial z}(\rho w) \cdot \frac{1}{2}dz\right] \cdot dxdy
\end{aligned}$$

$$= -\frac{\partial}{\partial z}(\rho w) \cdot dxdydz \tag{3.18}$$

The total mass change in the control volume $dv = dxdydz$ over the time is thus equal to:

$$\frac{\partial \rho}{\partial t}dxdydz = -\frac{\partial(\rho u)}{\partial x}dxdydz - \frac{\partial(\rho v)}{\partial y}dxdydz - \frac{\partial(\rho w)}{\partial z}dxdydz \tag{3.19}$$

$$\frac{\partial \rho}{\partial t} = -\frac{\partial(\rho u)}{\partial x} - \frac{\partial(\rho v)}{\partial y} - \frac{\partial(\rho w)}{\partial z} \tag{3.20}$$

Equation (3.20) is the same as Eq. (3.13), a general expression of the mass conservation of fluid flow.

For steady flows, Eq. (3.13) becomes:

$$\frac{\partial(\rho u_j)}{\partial x_j} = 0 \tag{3.21}$$

If considering incompressible fluids [i.e., the fluid density in the volume does not change during a flow process; however, the density may still be a function of space (x, y, z)], Eq. (3.13) can be expressed as:

$$\frac{\partial(\rho u_j)}{\partial x_j} = 0 \tag{3.22}$$

Note that Eqs. (3.21) and (3.22) are exactly the same; however, Eq. (3.22) does not imply a steady state flow, i.e., other variables such as velocity and temperature may still be able to vary with time. If assuming a constant fluid density, Eq. (3.22) can be further simplified as:

$$\frac{\partial u_j}{\partial x_j} = 0 \tag{3.23}$$

(2) **Momentum Equations (Momentum Conservation)**

$$\frac{\partial}{\partial t}(\rho u_i) + \frac{\partial}{\partial x_j}(\rho u_j u_i) = -\frac{\partial p}{\partial x_i} + \frac{\partial t_{ji}}{\partial x_j} + \rho F_i \tag{3.24}$$

where, u_i and u_j are, respectively, the instantaneous velocity component in x_i and x_j direction; p is the instantaneous pressure; t_{ij} is the component of viscous stress tensor; and F_i is the volume force working on the fluid.

The equation can be better understood in physics if a control volume $dv = dx_1dx_2dx_3$ is multiplied to each term in Eq. (3.24). Using $i = 1$ as a demonstra-

tion, the first term on the left is called *dynamic term*, which represents the change of the momentum ($dm \times u_1 = \rho dv \times u_1$) over the time in the control volume in the x_1 (or X) direction,

$$\frac{\partial}{\partial t}(\rho u_1)dv = \frac{\partial}{\partial t}(\rho dv \cdot u_1) \tag{3.25}$$

The second term on the left can be rewritten as:

$$\begin{aligned}\frac{\partial}{\partial x_j}\left(\rho u_j u_1\right)dv &= \frac{\partial(\rho u_1 u_1)}{\partial x_1}dx_1dx_2dx_3 + \frac{\partial(\rho u_2 u_1)}{\partial x_2}dx_1dx_2dx_3 \\ &\quad + \frac{\partial(\rho u_3 u_1)}{\partial x_3}dx_1dx_2dx_3 \\ &= \partial[(\rho u_1 \cdot dx_2dx_3) \cdot u_1] + \partial[(\rho u_2 \cdot dx_1dx_3) \cdot u_1] \\ &\quad + \partial[(\rho u_3 \cdot dx_1dx_2) \cdot u_1] \\ &= \partial(\dot{m}_1 \cdot u_1) + \partial(\dot{m}_2 \cdot u_1) + \partial(\dot{m}_3 \cdot u_1)\end{aligned} \tag{3.26}$$

This represents the differences of the momentum entering and leaving the control volume, respectively, through the west ($x - 0.5dx$) and east ($x + 0.5dx$) surfaces, the south ($y - 0.5dy$) and north ($y + 0.5dy$) surfaces, and the bottom ($z - 0.5dz$) and top ($z + 0.5dz$) surface. $\dot{m}_1$, $\dot{m}_2$, $\dot{m}_3$ are the actual mass flow rates entering and leaving the cell (calculated using the velocity normal to the surfaces) at x, y, and z directions. Each of these mass flow rates may bring the momentum impacts to the control volume on the x_1 (or X) direction via the x_1 direction velocity component u_1 at each surface. The same physics is shown in the integral Eq. (3.11). This term is called *convection or advection term* as it is directly related to fluid flow.

The first term on the right of Eq. (3.24) is named *pressure term*, which represents the pressure forces acted on the cell surfaces that drive the flow. Equation (3.27) shows the pressure forces on the west and east surfaces that affect the momentum $\rho dv \cdot u_1$ in x_1 direction,

$$-\frac{\partial p}{\partial x_1}dv = -\frac{\partial p}{\partial x_1}dx_1dx_2dx_3 = -\partial\left(pdx_2dx_3\right) \tag{3.27}$$

The second term on the right of Eq. (3.24) is the impact from viscous stresses/forces at the surfaces of the volume and t_{ij} is viscous stress tensor.

$$\frac{\partial t_{j1}}{\partial x_j}dv = \partial(t_{11}dx_2dx_3) + \partial(t_{21}dx_1dx_3) + \partial(t_{31}dx_1dx_2) \tag{3.28}$$

where the first term on the right is the normal stress influence and the other two are the shear stress influence on the momentum $\rho dv \cdot u_1$ in x_1 direction.

According to the Stokes' law, the viscous stress tensor t_{ij} can be represented as:

$$t_{ij} = \mu\left(\frac{\partial u_i}{\partial x_j} + \frac{\partial u_j}{\partial x_i}\right) - \frac{2}{3}\mu\frac{\partial u_k}{\partial x_k}\delta_{ij} \tag{3.29}$$

where μ is the molecular dynamic viscosity. $\delta_{ij} = 1$ if $i = j$ (otherwise zero). Note that the relationship of Eq. (3.29) only works for Newtonian fluids (e.g., air and water). The general expression of the momentum Eq. (3.24) is applicable for all fluids but may have different stress-strain correlations that are attributed to inherent properties of fluids.

The last term on Eq. (3.24) represents the body force on each volume/cell, which can be gravity or magnetic force etc. If gravity is considered, this *source term* can be written as

$$\rho F_i dv = \rho dv \cdot g_i \tag{3.30}$$

where $F_i = g_i$ is the gravitational acceleration in the x_i direction.

(3) **Energy Equations (Energy Conservation)**

$$\begin{aligned}\frac{\partial}{\partial t}\left[\rho\left(e + \frac{u_i u_i}{2}\right)\right] + \frac{\partial}{\partial x_j}\left[\rho u_j\left(e + \frac{u_i u_i}{2}\right)\right] &= \frac{\partial}{\partial x_j}\left(u_i t_{ij}\right) \\ - \frac{\partial}{\partial x_j}\left(p u_j\right) + \rho F_i u_i - \frac{\partial q_i}{\partial x_i} + \rho q_{source}\end{aligned} \tag{3.31}$$

where e is the internal energy of the fluid (unit: kJ/kg), $\frac{u_i u_i}{2}$ is the instantaneous kinetic energy of the fluid, q_i is the heat flux in in x_i direction, and q_{source} is the energy source in the fluid.

The first term on the left of the equation is the dynamic term and is the total energy change within the control volume over the time. The second term is the convection term, representing the energy with flows entering/leaving the volume through the surfaces. The first term on the right is the energy from the mechanical work caused by surface stresses (e.g., frictions); the second term is the energy from the mechanical work by pressure (e.g., either pressure changes at the cell surfaces or cell volume change); the third one is the energy from the mechanical work done by the body force (e.g., gravity); the fourth one is the heat transfer across the surfaces of the volume; and the last one represents other energy sources in the volume (e.g., from chemical reactions inside the volume).

If using the enthalpy h to replace the internal energy e (i.e., the PV work is considered in the fluid total energy, which is common), Eq. (3.31) becomes

$$\begin{aligned}\frac{\partial}{\partial t}\left[\rho\left(h + \frac{u_i u_i}{2}\right)\right] + \frac{\partial}{\partial x_j}\left[\rho u_j\left(h + \frac{u_i u_i}{2}\right)\right] &= \frac{\partial}{\partial x_j}\left(u_i t_{ij}\right) + \rho F_i u_i \\ - \frac{\partial q_i}{\partial x_i} + \rho q_{source} + \frac{\partial p}{\partial t}\end{aligned} \tag{3.32}$$

Typically, the following terms are grouped as a source term for the energy equation,

$$\phi = \frac{\partial}{\partial x_j}\left(u_i t_{ij}\right) + \rho F_i u_i + \rho q_{source} + \frac{\partial p}{\partial t} \tag{3.33}$$

The right term 1, 2 and 4 are generally smaller than the heat transfer term $-\frac{\partial q_i}{\partial x_i}$ and thus neglected by many practical CFD software and simulations. Hence, $\phi = \rho q_{source}$. The change of instantaneous kinetic energy $\frac{u_i u_j}{2}$ is also smaller compared to either internal energy or enthalpy, and hence often ignored in the energy equation. The refined energy equation then becomes:

$$\frac{\partial(\rho h)}{\partial t} + \frac{\partial\left(\rho u_j h\right)}{\partial x_j} = -\frac{\partial q_i}{\partial x_i} + \phi \tag{3.34}$$

For ideal gases and incompressible fluids, the enthalpy of fluid can be calculated by:

$$h = C_p T \tag{3.35}$$

where C_p is specific heat at constant pressure (and usually treated as a constant), and T is the instantaneous fluid temperature. According to the Fourier's law, the conductive heat transfer in the fluid can be expressed as:

$$q_i = -\kappa \frac{\partial T}{\partial x_i} \tag{3.36}$$

where k is the thermal conductivity of fluid. Substituting (3.35) and (3.36) into (3.34) yields

$$\frac{\partial\left(\rho C_p T\right)}{\partial t} + \frac{\partial\left(\rho C_p u_j T\right)}{\partial x_j} = \frac{\partial}{\partial x_k}\left(\kappa \frac{\partial T}{\partial x_k}\right) + \phi \tag{3.37}$$

The flow governing Eqs. (3.13), (3.24) and (3.31) are generally called the Navier-Stokes equations. Equations (3.13), (3.24) and (3.37) forms a complete set of flow governing equations for ideal gases and incompressible fluids—two commonly encountered flows in fluid engineering applications, with five (5) equations for six (6) variables: u_1, u_2, u_3, p, T, ρ. Additional equation is required to enclose this problem mathematically. For ideal gases, it is the state equation,

$$p = \rho R T \tag{3.38}$$

where R is the ideal gas constant.

(a) *Instantaneous Governing Equations for Ideal Gas Flows*

$$\frac{\partial \rho}{\partial t} + \frac{\partial \left(\rho u_j\right)}{\partial x_j} = 0 \tag{3.39}$$

$$\frac{\partial (\rho u_i)}{\partial t} + \frac{\partial \left(\rho u_j u_i\right)}{\partial x_j} = -\frac{\partial p}{\partial x_i} + \frac{\partial t_{ji}}{\partial x_j} + \rho g_i \tag{3.40}$$

$$\frac{\partial \left(\rho C_p T\right)}{\partial t} + \frac{\partial \left(\rho C_p u_j T\right)}{\partial x_j} = \frac{\partial}{\partial x_k}\left(\kappa \frac{\partial T}{\partial x_k}\right) + \phi \tag{3.41}$$

$$p = \rho R T \tag{3.42}$$

(b) *Instantaneous Governing Equations for Incompressible Fluid Flows*

Equations (3.13), (3.24) and (3.37) can also be closed by using the incompressible assumption for fluids, where the fluid density ρ is assumed to be constant.

By substituting the t_{ij} expression (3.29) into Eq. (3.24) and taking into account the continuity Eq. (3.23) for incompressible fluids and assuming gravity is the only body force, the momentum Eq. (3.24) can be rewritten as

$$\begin{aligned}
\frac{\partial}{\partial t}(\rho u_i) + \frac{\partial}{\partial x_j}\left(\rho u_j u_i\right) &= -\frac{\partial p}{\partial x_i} + \frac{\partial}{\partial x_j}\left(\mu\left(\frac{\partial u_i}{\partial x_j} + \frac{\partial u_j}{\partial x_i}\right)\right) + \rho g_i \\
&= -\frac{\partial p}{\partial x_i} + \mu \frac{\partial}{\partial x_j}\left(\frac{\partial u_i}{\partial x_j}\right) + \mu \frac{\partial}{\partial x_j}\left(\frac{\partial u_j}{\partial x_i}\right) + \rho g_i \\
&= -\frac{\partial p}{\partial x_i} + \mu \frac{\partial}{\partial x_j}\left(\frac{\partial u_i}{\partial x_j}\right) + \mu \frac{\partial}{\partial x_i}\left(\frac{\partial u_j}{\partial x_i}\right) + \rho g_i \\
&= -\frac{\partial p}{\partial x_i} + \mu \frac{\partial}{\partial x_j}\left(\frac{\partial u_i}{\partial x_j}\right) + \rho g_i
\end{aligned} \tag{3.43}$$

Since the fluid density is treated as constant, the influence of fluid temperature variation on the density and then on the flow momentum, in terms of buoyancy, is decoupled. As a result, the Boussinesq buoyancy approximation is suggested to couple the momentum and energy equations. As a first order truncation, the Boussinesq buoyancy approximation presents the relationship between gas density and temperature as

$$\rho = \rho_o[1 - \beta(T - T_o)] \tag{3.44}$$

where ρ_o is the reference density at the reference temperature T_o. $\beta = 1/T$ is the coefficient of volume expansion of the fluid (unit: 1/K). Taking this into Eq. (3.43) and absorbing the constant $\rho_o g_i$ into the pressure term (because only the pressure difference matters), the momentum equation for incompressible fluids becomes

$$\begin{aligned}\frac{\partial}{\partial t}(u_i)+\frac{\partial}{\partial x_j}\left(u_j u_i\right) &= \frac{\partial}{\partial t}(u_i)+u_j\frac{\partial}{\partial x_j}(u_i)\\ &= -\frac{\partial p}{\rho\partial x_i}+\frac{\mu}{\rho}\frac{\partial}{\partial x_j}\left(\frac{\partial u_i}{\partial x_j}\right)-g_i\beta(T-T_o)\\ &= -\frac{\partial p}{\rho\partial x_i}+\nu\frac{\partial^2 u_i}{\partial x_j\partial x_j}-g_i\beta(T-T_o)\end{aligned} \tag{3.45}$$

where $\nu=\mu/\rho$ is the kinematic viscosity (unit: m^2/s).

Energy Eq. (3.37) can also be revised as

$$\frac{\partial T}{\partial t}+\frac{\partial\left(u_j T\right)}{\partial x_j}=\frac{\partial T}{\partial t}+u_j\frac{\partial T}{\partial x_j}=\frac{1}{\rho c_p}\frac{\partial}{\partial x_k}\left(\kappa\frac{\partial T}{\partial x_k}\right)+\frac{\phi}{\rho c_p} \tag{3.46}$$

The following is the complete set of governing equations for incompressible fluid flows with five (5) equations for five (5) variables: u_1, u_2, u_3, p, T.

$$\frac{\partial u_i}{\partial x_j}=0 \tag{3.47}$$

$$\frac{\partial u_i}{\partial t}+u_j\frac{\partial u_i}{\partial x_j}=-\frac{\partial p}{\rho\partial x_i}+\nu\frac{\partial^2 u_i}{\partial x_j\partial x_j}-g_i\beta(T-T_o) \tag{3.48}$$

$$\frac{\partial T}{\partial t}+u_j\frac{\partial T}{\partial x_j}=\frac{1}{\rho c_p}\frac{\partial}{\partial x_k}\left(\kappa\frac{\partial T}{\partial x_k}\right)+\frac{\phi}{\rho c_p} \tag{3.49}$$

(4) **General Scalar Transport Equation (Mass Conservation)**

If a concentration of particular species (other than the domain fluid) is concerned in the flow, such as the concentrations of moisture and pollutant in the air, the concentration transport equation need be resolved. The concentration equation fundamentally is a mass transport or conservation equation, which can be expressed in a general scalar transport equation form as below:

$$\frac{\partial(\rho C)}{\partial t}+\frac{\partial\left(\rho u_j C\right)}{\partial x_j}=\frac{\partial}{\partial x_k}\left(\alpha\frac{\partial(C)}{\partial x_k}\right)+q_{source} \tag{3.50}$$

where, C is the instantaneous scalar variable such as species concentration, α is the molecular diffusion coefficient for the scalar, and q_{source} is the source term. Note that Eq. (3.50) is very similar to the energy Eq. (3.37). Using contaminant concentration as an example, if the unit of C is kg_c/kg_{air}, the integration of the first term over the volume dv provides

$$\frac{\partial}{\partial t}(\rho C)dv=\frac{\partial}{\partial t}(\rho dv\cdot C)\quad\left(\text{unit: } kg_c/s\right) \tag{3.51}$$

This is the change rate of the contaminant mass in dv. This change is due to

(1) the contaminant mass entering and leaving dv with the flow:

$$\begin{aligned}\frac{\partial}{\partial x_j}\left(\rho u_j C\right)dv &= \frac{\partial(\rho u_1 C)}{\partial x_1}dx_1dx_2dx_3 + \frac{\partial(\rho u_2 C)}{\partial x_2}dx_1dx_2dx_3 \\ &\quad + \frac{\partial(\rho u_3 C)}{\partial x_3}dx_1dx_2dx_3 \\ &= \partial[(\rho u_1 \cdot dx_2dx_3)\cdot C] + \partial[(\rho u_2 \cdot dx_1dx_3)\cdot C] \\ &\quad + \partial[(\rho u_3 \cdot dx_1dx_2)\cdot C] \\ &= \partial(\dot{m}_1 \cdot C) + \partial(\dot{m}_2 \cdot C) + \partial(\dot{m}_3 \cdot C) \quad \left(\text{unit: } kg_c/s\right)\end{aligned} \tag{3.52}$$

(2) the dispersion (or diffusion) at the volume surfaces due to the concentration gradient:

$$\begin{aligned}\frac{\partial}{\partial x_k}\left(\alpha\frac{\partial C}{\partial x_k}\right)dv &= \frac{\partial}{\partial x_1}\left(\alpha\frac{\partial C}{\partial x_1}\right)dv + \frac{\partial}{\partial x_2}\left(\alpha\frac{\partial C}{\partial x_2}\right)dv + \frac{\partial}{\partial x_3}\left(\alpha\frac{\partial C}{\partial x_3}\right)dv \\ &= \left(\alpha\frac{\partial C}{\partial x_1}dA\right)_{east} - \left(\alpha\frac{\partial C}{\partial x_1}dA\right)_{west} \\ &\quad + \left(\alpha\frac{\partial C}{\partial x_2}dA\right)_{north} - \left(\alpha\frac{\partial C}{\partial x_2}dA\right)_{south} \\ &\quad + \left(\alpha\frac{\partial C}{\partial x_3}dA\right)_{top} - \left(\alpha\frac{\partial C}{\partial x_3}dA\right)_{bottom}\end{aligned} \tag{3.53}$$

The molecular diffusion coefficient α has the same unit as dynamic viscosity μ, kg/(m s). $\alpha\frac{\partial C}{\partial x_i}dA$ is the diffusion at the surfaces due to the concentration gradient, and the unit of this is

$$\frac{kg_{air}}{m\cdot s}\cdot\frac{kg_c}{kg_{air}}\cdot\frac{1}{m}\cdot m^2 = \frac{kg_c}{s} \tag{3.54}$$

(3) the source term $q_{source}\cdot dv$ in unit of kg_c/s (i.e., either source or sink of the contaminant within the volume dv. Note that the scalar unit will vary according to the unit of the source term.

(5) **Uniform Expression of Flow Governing Equations**

The governing equations of incompressible flow (3.47)–(3.49) and the scalar transport Eq. (3.50) can be generalized into the following form:

$$\frac{\partial(\rho\phi)}{\partial t} + \frac{\partial\left(\rho U_j\phi\right)}{\partial x_j} = \frac{\partial}{\partial x_j}\left(\Gamma_{\phi,eff}\frac{\partial\phi}{\partial x_j}\right) + S_\phi \tag{3.55}$$

Table 3.1 Formula for the general form Eq. (3.55)

Equation	ϕ	$\Gamma_{\phi,\text{eff}}$	S_ϕ
Continuity	1	0	0
Momentum	U_i	μ	$-\frac{\partial p}{\partial x_i} - \rho\beta(T - T_\infty)g_i$
Temperature	T	$\frac{\mu}{Pr}$	S_T
Concentration	C	$\frac{\mu}{Sc}$	S_C

where ϕ represents the physical variable in question, as shown in Table 3.1. The equation has dynamic, convection, diffusion and source terms.

When selecting proper equations to be computed, appropriate assumptions (e.g., steady state and/or impressible state) and case simplifications (e.g., 2-D and constant coefficients) should be determined first. This will identify how many variables and equations to solve. Additional equations for temperature and concentrations should be included whenever the physics of flow requires so. More equations selected will impose extra computing sophistication and costs. Boundary (and initial) conditions are mandatory for all these equations as will be described in Chap. 6.

3.4 Transport Equations for Particle and Droplet

Predicting particle and droplet transport behaviors in the air is essentially a simulation of air-particle two-phase flows with continuous gas phase of air and dispersed solid/liquid phase of particles/droplets. To simulate the movement of continuous air, the flow governing Eqs. (3.47)–(3.49) in Eulerian-form are solved. To predict the transport of dispersed particles and droplets in the air, three kinds of models are usually available (Liu and Zhai 2007):

- Lazy particle model
- Isothermal particle model
- Vaporizing droplet model.

The lazy particle model does not solve the particle trajectories directly and thus does not produce individual particle velocities. It simply follows the continuous-phase velocity (streamline) at each point of the flow field—a model that is tracer-like (hence also called the 'tracer' model). The model does not handle either size or temperature of particles, and cannot undergo any physical process (e.g., solidification and vaporization) except turbulent dispersion. Lazy particles will not affect the continuous-phase solution. The distributed concentration of lazy particles can be simulated by solving the same transport equation for gas-phase contaminants, i.e. Eq. (3.50). Lazy particle model may be appropriate for small particles with quasi-gaseous compounds that have similar molecular weights to the elements in air and when particle-particle interaction is not concerned. Due to its simplicity, the model has been broadly used for indoor and outdoor particle study.

The isothermal particle model predicts particle trajectories and velocities by solving additional Lagrangian transport equations for particles without considering particle thermal effect. As a result, simulated particles do not change their sizes during the transport and there is no exchange of heat and mass between continuous and dispersed phases. The model can be applicable to many solid particle pollutants, such as, tobacco smoke particulates, soot, and fibers.

When liquid particles (droplets) are simulated, the evaporation effect could be important so that the Lagrangian particle transport equations must consider the exchange of mass and heat (besides momentum) between dispersed and continuous phases. This vaporizing droplet model represents the true physics of droplet dispersion but also complicates the simulation. Evaporation is commonly included in fire extinguishing modeling when water sprinklers are used, but very few researchers take this into account in air quality study because usually less mass and heat transfer occur during regular room-temperature droplet transport process. However, this small mass and heat transfer could be significant, such as for predicting the fate of droplets carrying viruses or bacteria.

Most studies take the liberty of deciding appropriate (or convenient) simulators to predict particle and droplet transport behaviors. Generally, lazy particle model is employed if one thinks that the particle size is relatively small and the distributed contaminant concentration is the major concern; otherwise, isothermal particle model will be utilized. Vaporizing droplet model is the least used model due to the complexity of the model unless special considerations need be taken into account. It is unclear which model is the most effective and efficient for a certain particle or droplet or how large is the difference in the results predicted by different models. It is also uncertain under what circumstances the air-particle interaction and droplet mass change must be considered as they influence the motion of particles and droplets in the space. The answers to these questions are affected by many factors, such as, simulation accuracy requirement, computing cost affordability, particle sizes, and environment conditions, etc. The following sections attempt to provide some practical particle-size-based criteria for selecting an appropriate particle simulation method.

(1) **Theoretical Analysis**

- ***General Particle Transport Equation***

When using the Lagrangian method, the trajectory of each particle in the air can be computed by solving the momentum equation based on Newton's second law,

$$\frac{d(m\vec{v})}{dt} = \sum \vec{F} \tag{3.56}$$

and

$$\frac{d\vec{X}_p}{dt} = \vec{v} \tag{3.57}$$

where $\vec{v}$ is the particle velocity, m is the particle mass, $\sum \vec{F}$ stands for the total forces acted on the particle, and $\vec{X}_p$ is the co-ordinates of the particle. Momentum is transferred between air and particles through inter-phase drag and lift forces that can be divided into, but not limited to, the following parts: the drag force, pressure gradient and buoyancy forces, unsteady forces that include Basset force and virtual mass force, Brownian force, and body forces such as gravity force (Crowe et al. 1998). For particles with a certain size and density, some of the forces may be very small compared to others, and thus can be ignored. For most spherical particles, the particle motion equation can be simplified as (Crowe et al. 1998):

$$\frac{d(m\vec{v})}{dt} = \frac{1}{2} C_D \frac{\pi D^2}{4} \rho_a (\vec{u} - \vec{v}) |\vec{u} - \vec{v}| + m\vec{g} \tag{3.58}$$

where $\vec{v}$ is the particle velocity, $\vec{u}$ is the local air velocity, D is the particle diameter, ρ_a is the air density, and C_D is the drag coefficient. Equation (3.58) only includes the most important drag force and gravity force acted on a particle, which is appropriate for particles with size above 1 μm and density above the order of $1\ 0^3$ kg/m^3 (Jiang 2002).

By introducing the particle Reynolds number $Re_r = \frac{\rho_a D|\vec{u}-\vec{v}|}{\mu_a}$ and the spherical particle mass $m = \frac{1}{6}\rho_p \pi D^3$, Eq. (3.58) can be written as

$$\frac{d\vec{v}}{dt} = \frac{18\mu_a}{\rho_p D^2} \frac{C_D Re_r}{24} (\vec{u} - \vec{v}) + \vec{g} = \frac{18\mu_a}{\rho_p D^2} f(\vec{u} - \vec{v}) + \vec{g} \tag{3.59}$$

where μ_a is the air viscosity and ρ_p is the particle density. $f = \frac{C_D Re_r}{24}$ is defined as drag factor. One accurate correlation for f over the entire sub-critical Reynolds number range was developed by Clift and Gauvin (1970):

$$f = 1 + 0.15 Re_r^{0.687} + 0.0175 \times \left(1 + 4.25 \times 10^4 Re_r^{-1.16}\right)^{-1} \tag{3.60}$$

Figure 3.4 illustrates the relationship between f and Re_r in Eq. (3.60), which shows that f approaches to 1 as $Re_r < 1$.

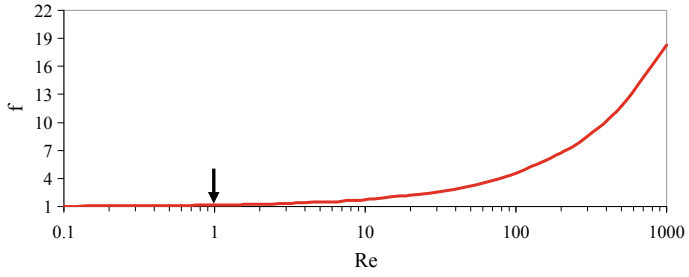

Fig. 3.4 Relationship between f and Re_r in Eq. (3.60)

- ***Movement of Particle without Evaporation***

For spherical particles without considering mass change, particle diameters remain constant during the transmission. This analyze discusses the transport behaviors of such particles of different sizes in both low and high Reynolds flows.

(1) *Low Reynolds Flow ($Re_r < 1$)*

Since the drag factor f in Eq. (3.59) approximates to one when $Re_r < 1$, Eq. (3.59) can be expressed as:

$$\frac{d\vec{v}}{dt} = \frac{(\vec{u} - \vec{v})}{\tau_v} + \vec{g} \tag{3.61}$$

where $\tau_v = \frac{\rho_p D^2}{18\mu_a}$ is defined as the particle momentum (velocity) response time (second) and is constant for a certain particle with constant diameter.

To simplify the theoretical analysis, a two-dimensional air-particle flow is assumed in a x-y Cartesian coordinate system. Equation (3.61) then becomes

$$\begin{cases} \frac{dv_x}{dt} = \frac{u_x - v_x}{\tau_v} \\ \frac{dv_y}{dt} = \frac{u_y - v_y}{\tau_v} - g \end{cases} \tag{3.62}$$

By assuming a constant airflow velocity $\vec{u} = u_x\vec{i} + u_y\vec{j}$ and a zero initial particle velocity, the analytical solutions to Eq. (3.62) can be obtained

$$\begin{cases} v_x = u_x\left(1 - e^{-t/\tau_v}\right) \\ v_y = \left(u_y - \tau_v g\right)\left(1 - e^{-t/\tau_v}\right) \end{cases} \tag{3.63}$$

As a result, $v_x = u_x$ and $v_y = u_y - \tau_v g$ if $t = \infty$, and $v_x = 63\%u_x$ and $v_y = 63\%\left(u_y - \tau_v g\right)$ if $t = \tau_v$. Hence, the particle momentum response time τ_v indicates how fast the particle can reach the air velocity and respond to the air velocity changes. Figure 3.5 presents the change of particle momentum response time with particle diameters in the air. If τ_v is adequately small, particles can easily follow the air velocity so that lazy particle model is appropriate. Conversely, if τ_v is significantly large, the time needed to reach the air velocity is much longer than the time needed for particle to fall on floor and thus a free dropping calculation may be sufficient.

To find the critical particle momentum response times or particle diameters, the Stokes Number is introduced

$$St_v = \frac{\tau_v}{\tau_F} \tag{3.64}$$

where τ_F is the characteristic time of a flow field that represents the shortest time for a certain particle to be caught by obstructions. For indoor particles dispersing in a ventilated space as illustrated in Fig. 3.6, τ_F can be calculated via

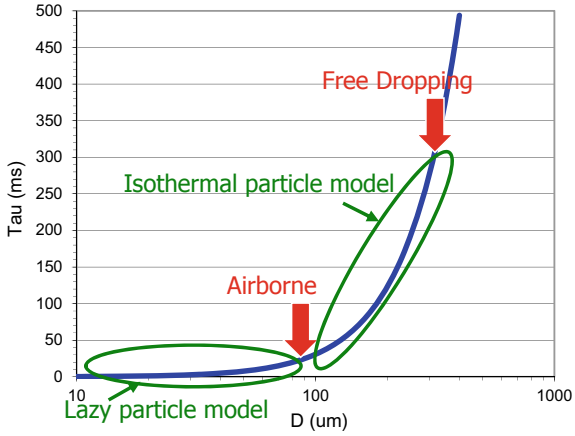

Fig. 3.5 Relationship between τ_v and particle diameter D

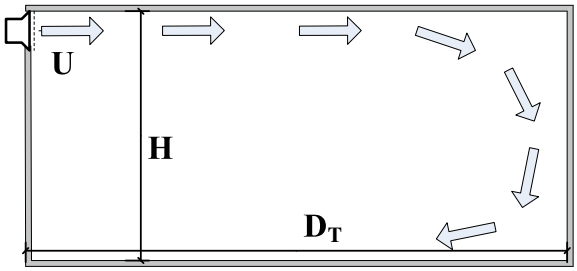

Fig. 3.6 Characteristic time for a ventilated indoor space

$$\tau_F = \min\left(D_T/U, \sqrt{2H/g}\right) \tag{3.65}$$

where D_T is the depth of the room, U is the vent inlet air velocity, H is the height of the room, g is the gravitational acceleration.

If the Stokes Number is far less than one, i.e., the particle momentum response time is much less than the characteristic time associated with the flow field, the particles will have ample time to respond to and follow the changes in flow velocity. As a result, the particle and fluid velocities can be treated as velocity equilibrium and lazy particle model can be applied. In contrast, if the Stokes Number is far larger than one, the particle will essentially have no time to respond to the fluid velocity changes before they are caught by building envelopes. For particles with St_v number in between, Lagrangian particle transport equation must be solved.

(2) *High Reynolds Flow ($Re_r > 1$)*

When $Re_r > 1$, $f = C_D Re_r/24$ is not equal to one any more. Equation (3.59) becomes

$$\frac{d\vec{v}}{dt} = \frac{(\vec{u} - \vec{v})}{\tau_v'} + \vec{g} \tag{3.66}$$

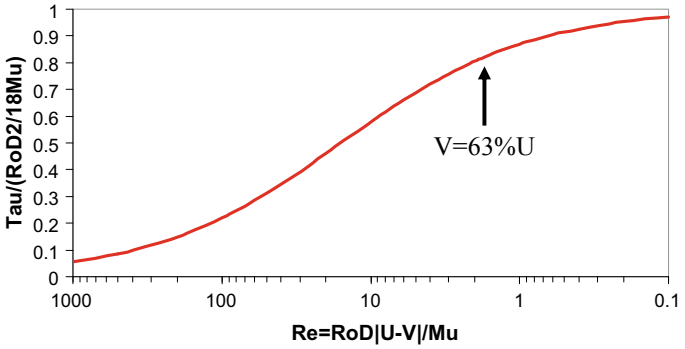

Fig. 3.7 Variation of $\tau_v'/\left(\rho_p D^2/18\mu_a\right) = 1/f$ with $Re_r = \rho_a D|\vec{u} - \vec{v}|/\mu_a$

where $\tau_v' = \frac{\rho_p D^2}{18\mu_a}\frac{1}{f}$ is defined as the modified particle momentum (velocity) response time. Because $f > 1$ for the entire subcritical Reynolds number range according to Eq. (3.60), τ_v' is always smaller than τ_v. Figure 3.7 illustrates the variation of $\tau_v'/\left(\rho_p D^2/18\mu_a\right) = 1/f$ with $Re_r = \rho_a D|\vec{u} - \vec{v}|/\mu_a$. When particle and air have relatively large velocity difference thus large Re_r, a large drag factor f occurs to change the particle velocity to follow the air speed, which corresponds to a small "local" modified particle momentum response time τ_v'. When the particle speed approaches the air velocity, less drag force is imposed on the particle, which leads to longer time to further alter its speed towards that of the free air. To be consistent with low Reynolds flow and produce a simple justification criterion, a "local" $\tau'_{V=63\%U}$ is used to represent the total time for a particle released from rest to achieving 63% of the free stream velocity. This number overestimates the real time but reflects its magnitude. By using the Stokes number $St_v = \tau'_{V=63\%U}/\tau_F$, the same conclusions as for low Reynolds flows can be reached for high Reynolds flows.

- ***Movement of Particle with Evaporation***

For spherical particles with evaporation, their diameters keep varying due to evaporation during the transmission. Besides the particle momentum Eq. (3.59), an additional equation that describes such mass change of the droplet must be solved. One of the representative droplet mass change equations was developed by Ludwig et al. (2004):

$$\frac{dm_p}{dt} = -\pi D_p \frac{K_v}{Cp_v} Nu \ln(1 + B_m) \tag{3.67}$$

where m_p is the droplet mass, D_p is the droplet diameter, K_v is the thermal conductivity of droplet vapor, Cp_v is the specific heat capacity of droplet vapor. Nu is the Nusselt number, determined from the following correlation:

$$Nu = 2\left(1 + 0.3Re_r^{0.5} Pr^{0.33}\right)F \tag{3.68}$$

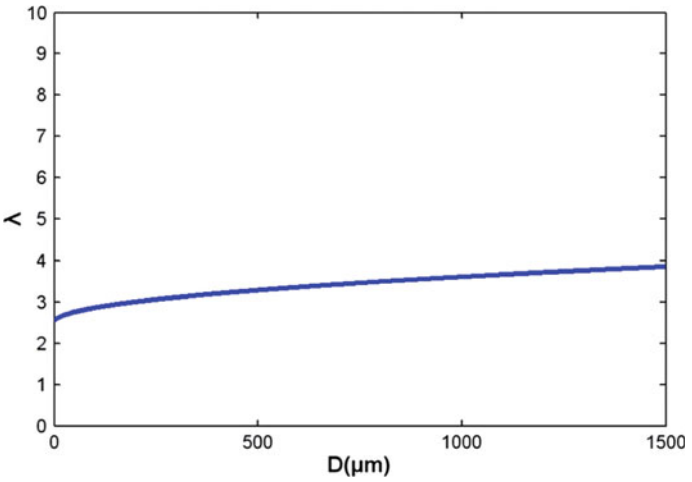

Fig. 3.8 Evaporation constant λ versus water droplet diameter

where *Pr* is the laminar Prandtl number of air and F is the Frossling correction for mass transfer given by $F = \ln(1 + B_m)/B_m$. B_M is the mass transfer number, which represents the "driving force" in the mass transfer process, and is defined by:

$$B_M = \left[\frac{Y_{vs} - Y_{v\infty}}{1 - Y_{vs}} \right] \tag{3.69}$$

where $Y_{v\infty}$ is the mass fraction of droplet vapour in the air surrounding the droplet, and Y_{vs} is the mass fraction of droplet vapour at the surface of droplet and can be calculated via:

$$Y_{vs} = \left[1 + \left(\frac{P}{P_{vs}} - 1 \right) \frac{W_a}{W_v} \right]^{-1} \tag{3.70}$$

where P is the total pressure of air surrounding droplet, P_{vs} is the partial pressure of droplet vapour at the surface of droplet at the saturation conditions defined by the droplet temperature, W_a is the molecular weight of air, and W_v is the molecular weight of droplet vapour.

Equation (3.67) can be rewritten as

$$D_p \frac{dD_p}{dt} = -2 \frac{K_v}{Cp_v} \frac{Nu}{\rho_p} \ln(1 + B_m) = -\frac{\lambda}{2} \tag{3.71}$$

Numerical experiments show that $\lambda = 4 \frac{K_v}{Cp_v} \frac{Nu}{\rho_p} \ln(1 + B_m)$ is almost constant for a certain droplet vapor under typical room conditions (and so called the evaporation constant). Figure 3.8 verifies that λ increases less than 1.7 times when water droplet diameter changes from nearly 0 to 1500 μm with a droplet temperature of 310 K.

Integrating Eq. (3.71) with the evaporation constant thus provides

$$D^2 = D_0^2 - \lambda t \tag{3.72}$$

This is a popular form of the evaporation equation that has been extensively used in the past. The evaporation lifetime of a droplet is then defined as the time needed to change droplet diameter from D_0 to $D = 0$

$$\tau_m = \frac{D_0^2}{\lambda} \tag{3.73}$$

To quantify the relative evaporation speed of a droplet, a new index—evaporation effectiveness (EE) number—has been introduced

$$EE = \frac{\tau_m}{\tau_F} = \frac{D_0^2}{\lambda \tau_F} \tag{3.74}$$

If $EE \ll 1$, i.e., the droplet evaporation time is much less than the characteristic time associated with the flow field, the droplet evaporates and disappears very fast. Therefore, such droplets can be treated as airborne. Conversely, if $EE \ll 1$, the droplet will be caught by building enclosures before it barely changes its diameter through evaporation. In this case, the evaporation-free particle model will be sufficient. For all other cases with EE numbers falling in between, a particle model with evaporation has to be considered.

(2) **Numerical Experiments**

- ***Case Descriptions***

Figure 3.9 shows the two-dimensional ventilated room modeled with CFD. The room is 10 m long and 3 m high with supply inlet at the top left corner of the room and exhaust vent at the bottom right corner. The supply air velocity is 0.1 m/s. A still particle or droplet is released from the center of the room at height = 1.8 m (nose level). The flow characteristic time for this case is 0.6 s, which is the dropping time of a free object from 1.8 m.

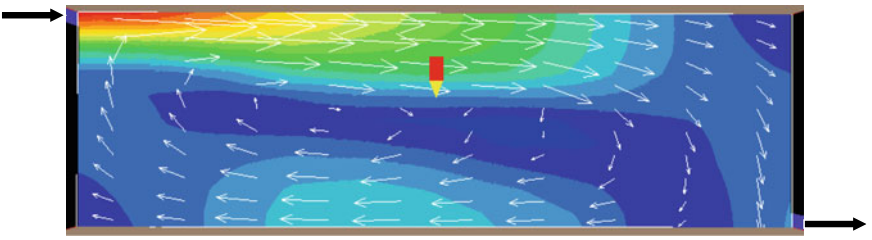

Fig. 3.9 Simulated flow pattern of the ventilated room

- ***Particle without Evaporation***

Figure 3.10 shows the predicted trajectories of isothermal particles with different diameters by CFD. For comparison, the 1500 s trajectory of lazy particles released at the same location is illustrated, which represents the streamline of airflow through the source location. The 20 μm particle can be seen as airborne because it never falls onto the floor and tends to follow the airflow. The 40 μm particle will hit the floor after 37 s while the 100 μm particle will do so after 7.2 s. For both cases, the influence of airflow on particle trajectories is perceivable. The trajectories and falling time of the 1500 μm particle and 10,000 μm particle are almost identical. The 10,000 μm-particle is almost like an object in free-fall since the dropping time is very close to 0.6 s—the flow characteristic time. Therefore, for typical room conditions, 20 and 1500 μm can be used as critical diameters between airborne particles, Lagrangian isothermal particles and free dropping particles, which correspond to the Stokes numbers of 0.001 and 10, respectively, as demonstrated in Table 3.2.

- ***Particle with Evaporation***

Figure 3.11 shows the predicted trajectories of vaporizing particles (droplets) with different diameters by CFD. In the simulation, the room air temperature remains 293 K, while the initial droplet temperature is the same as the normal human body temperature of 310 K. The results show that the 40 μm droplet completely evaporates to the air after 2.18 s before it starts to spread while the 100 μm droplet takes 12.2 s to fully evaporate. The 300 μm droplet falls on the floor after 2.31 s during which

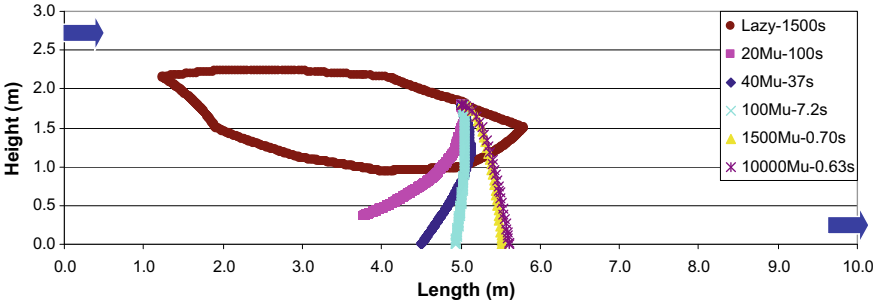

Fig. 3.10 Predicted trajectories of isothermal particles with different sizes in a ventilated room

Table 3.2 Model selection criteria for simulating isothermal particle movement in the air

Stokes number	Category	Critical St_v	Corresponding D
$St_v \ll 1$	Lazy particle	$St_{v,cr} = 0.001$	$D_{cr} = 20\ \mu m$
$St_v \approx 1$	Isothermal particle	$0.001 < St_{v,cr} < 10$	$20\ \mu m < D < 1500\ \mu m$
$St_v \gg 1$	Free dropping particle	$St_{v,cr} = 10$	$D_{cr} = 1500\ \mu m$

Note The corresponding D is calculated with typical building parameters $D_T = 10$ m, H = 3 m, U = 0.1 m/s, $\rho_p = 1000\ kg/m^3$

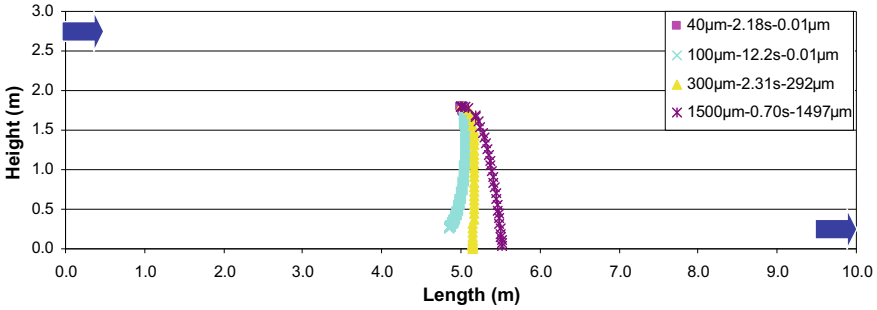

Fig. 3.11 Predicted trajectories of vaporizing particles with different sizes in the ventilated room

time the droplet diameter is barely changed. The 1500 μm droplet further exhibits the characteristics of an object in free-fall with less influence from airflow. Table 3.3 calculates the corresponding evaporation effectiveness numbers to the critical droplet diameters under typical room conditions and indicates the appropriate models for simulating droplet with different sizes.

(3) **Summary**

Different particle and droplet CFD models provide different simulation results in which the size of particle and droplet is a critical justification factor. By analyzing the particle and droplet momentum and mass conservation equations, two practical indices—the Stokes number and the Evaporation Effectiveness number are proposed to be applied as simple criteria to determine appropriate CFD models for particle and droplet prediction. The case studies provide the rules of thumb that can be used by building application engineers to guide their engineering simulations of indoor air quality under typical room conditions, as summarized in Fig. 3.12.

According to Fig. 3.12, the bacteria and viral particles can be represented fairly accurately by the lazy model because their diameters are far less than 20 μm as shown in Fig. 3.13. Bio-aerosols with nuclei that are free from evaporation, such as droplets produced during coughing or sneezing, can also be reasonably simulated by the lazy model due to their small sizes. For larger-size solid particles such as pollens and plant spores that usually have diameters of over 20 μm, the isothermal particle model may be necessary. The vaporizing droplet model is imperative for

Table 3.3 Model selection criteria for simulating vaporizing particle movement in the air

EE number	Category	Critical EE	Corresponding D
$EE \ll 1$	Lazy particle	$EE = 0.01$	$D_{cr} = 40\ \mu m$
$EE \approx 1$	Vaporizing particle	$0.01 < EE < 10$	$40\ \mu m < D < 1500\ \mu m$
$EE \gg 1$	Isothermal particle	$EE = 10$	$D_{cr} = 1500\ \mu m$

Note The corresponding D is calculated with typical building parameters $D_T = 10$ m, $H = 3$ m, $U = 0.1$ m/s, $\rho_p = 1000$ kg/m^3, RH = 40%, $T = 20$ °C

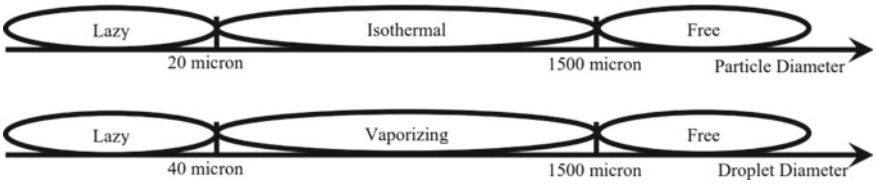

Fig. 3.12 Rules of thumb for selecting models to predict indoor particle and droplet transport

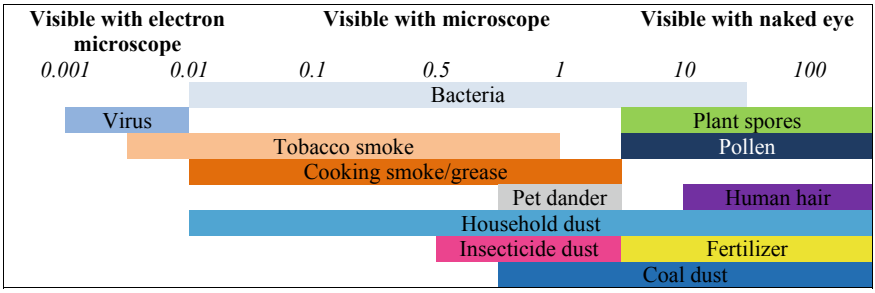

Fig. 3.13 Typical size ranges (in micron) of indoor air pollution particles

modeling droplets from sprinklers during fire extinguishing scenarios because of the large water droplet sizes. In practice, to be safe/accurate, 5 μm is also commonly used as a critical size to judge whether a Lagrangian model is needed. Although the rules of thumb provides the initial guidance on model selection, identifying a suitable model may still require specific (and sometime iterative) investigations that consider simulation goals, computing cost and affordability, and actual particle and environment conditions.

Practice-3: Indoor Airflow and Heat Transfer

Example Project: Air distribution inside a hospital operating room (OR)

Background:

The goal of the air distribution inside a hospital operating room (OR) is to protect the patient and staff from cross-infection while maintaining occupant comfort and not affecting the facilitation of surgical tasks. However, a source of contamination bypasses HEPA installations in every OR, this source being the surgical staff themselves and the particles stirred up by their movement (Cook and Int-Hout 2009). Therefore, air motion control must be used to maximize air asepsis.

In hospital ORs, using HEPA-filtered air and vertical (downward) laminar airflow is typical. ASHRAE Standard 170-2008 (ASHRAE 2008) requires that ventilation be

Table 3.4 Laboratory experiment specifications

Room dimensions	6.1 m × 5.8 m × 2.9 m
Diffuser dimensions	2.44 m × 3.05 m
Diffuser coverage area	7.06 m^2
Air change rate	31.6
Nominal face velocity	0.127 $m^3/s\ m^2$
Room air temperature	20 °C
Supply air temperature	18.3 °C
Room pressurization	+2.5 Pa

provided from the ceiling in a downward direction concentrated over the patient and surgical team. The area of the primary ventilation air diffusers must extend at least 305 mm beyond each side of the surgical table. It also requires that air is exhausted from at least two grilles on opposing sides of the room near the floor. It requires the use of non-aspirating, Group E outlets that provide a unidirectional flow pattern in the room (aka laminar flow diffusers). This study applied a computational fluid dynamics (CFD) tool to predict the flow pattern in a representative OR environment with standard air flow settings (Zhai and Osborne 2013).

Simulation Details:

The CFD model was built according to the full-scale laboratory experiment. The same diffuser specifications and air change rate per hour (ACH) as tested in the experiment were used in the CFD model, as well as the same room and equipment and occupant conditions, as shown in Table 3.4 and Fig. 3.14. These objects and heat gain values were chosen based on detailed on-site OR studies and measurements (Zhai et al. 2013). The equipment thermal loads as well as temperature of the patient's wound and skin can be seen in Table 3.5. Table 3.6 indicates the sizes of all of the objects in the room.

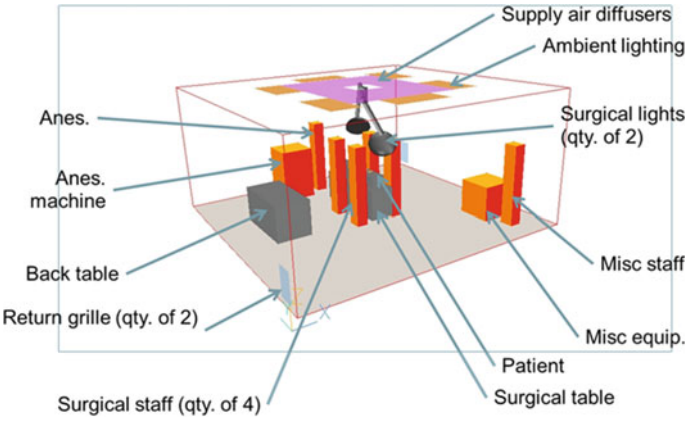

Fig. 3.14 Base CFD model setup

(a) **Geometry Generation:**

Melikov and Kaczmarczyk (2007) discussed the importance of detailed indoor objects such as human body on indoor airflow characteristics and indicated the local impacts of most details of indoor objects. Focusing on the general indoor airflow patterns and interactions between patient and medical staffs, this study simplified the simulation of indoor subjects such as human bodies and equipment as rectangular geometries (except the surgical lighting) with exact heat sources as tested. This practice facilitates the generation of high-quality meshes and therefore improves both speed and accuracy of the simulations.

(b) **Mesh Generation**

The example OR case was modeled using a rectangular Cartesian grid, which maps well to typical OR geometry. Local grid refinement was implemented near critical spaces and objects such as walls, inlets and persons. The results of a CFD simulation are highly dependent on the quality of the computational grid. The grid refinement study was conducted on the following grids: 70 × 58 × 45 (180 k cells), 87 × 73 × 57 (362 k cells), 106 × 91 × 70 (675 k cells), 124 × 111 × 86 (1.2 M cells), 155 × 142 × 108 (2.4 M cells). Figure 3.15 demonstrates the finest grid distribution.

Table 3.5 Laboratory thermal loads

Object	Qty	Heat gain (W)	Temperature (°C)
Manikins—male	2	80	
Manikins—female	4	68	
Anesthesia machine	1	100	
Surgical lights	2	250	
Monitor	1	200	
Ambient lights	6	128	
Patient wound	1		25.6
Patient skin	2		27.4

Table 3.6 Room object dimensions

Object	Qty	Dimensions (m)
Surgical table	1	0.54 × 1.88 × 0.66
Back table	1	0.76 × 1.52 × 0.76
Anesthesia machine	1	0.76 × 0.76 × 1.2
Surgical lighting	2	0.58 diameter
Misc. equipment (monitor)	1	0.76 × 0.76 × 0.76
Surgical staff	6	0.25 × 0.30 × 1.75
Patient body	1	0.30 × 1.60 × 0.25

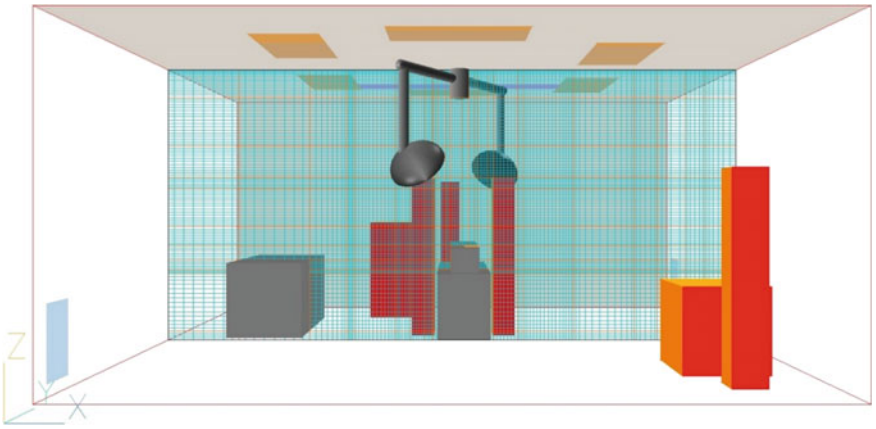

Fig. 3.15 Grid refinement case: 2.4 M cells

(c) **Solver and Models**

Both RANS and LES CFD methods were tested for this example case. While advanced CFD modeling techniques such as Large Eddy Simulation (LES) provide substantial benefits, the currently available RANS technologies have proven to be adequate for modeling the steady-state characteristics of the hospital operating room air distribution. In the RANS CFD solution methodology, the RNG $k-\varepsilon$ turbulence model (Yakhot and Orszag, 1986) was employed as suggested by Zhang et al. (2007). Details about these models will be introduced in Chap. 4 "Select Turbulence Modeling Method".

(d) **Boundary Conditions/Object Modeling**

Most indoor objects such as persons and equipment were specified straightforwardly using the standard wall/block boundary condition methods. Inlet boundary condition modeling is critical to accurate CFD modeling of indoor environments, as the inlet boundary condition is the primary source of momentum that is responsible for the overall room air distribution pattern. Srebric and Chen (2002) performed a comprehensive analysis of diffuser boundary conditions to determine appropriate simplified boundary conditions, and the box and momentum method have been determined to be the most appropriate models for the diffusers that were applied in this study. The momentum method was used in this example since it was recommended by Chen and Srebric (2002) for the grille diffuser that is similar to the non-aspirating diffuser type.

Results and Analysis:

(a) **Convergence/Grid Independence**

The simulation was considered converged when the sums of residual errors in the mass, momentum, energy, and turbulence-model equations, respectively, reach a pre-defined level (i.e., 0.1%). The grids of different sizes were evaluated using the

normalized root mean squared error (NRMSE) of the CFD model results with different grids (Wang and Zhai 2012) that will be described in Chap. 9 "Analyze Results". Figure 3.17 shows the NRMSE of the predicted U and W direction velocity at the four measure poles (1–4) across the center axis of the room (2.88 m) (shown in Fig. 3.16), between the 180 K (and 362 K) meshes and the 675 K mesh. It reveals that there is generally a great improvement in error with the 362 K mesh, and the computational error is typically below 10%, and absolutely below 30%. Based on these, and in order to minimize the simulation time, the 362 K mesh could be used for various engineering parametric simulations.

(b) **Model Validation**

The simulation replicates the airflow pattern as observed in the lab experiment (Zhai et al. 2013): an inward curvature of the airflow to the center of the jet stream, as seen in Fig. 3.18. This behavior reduces the overall coverage area and could pose a contamination risk to the patient.

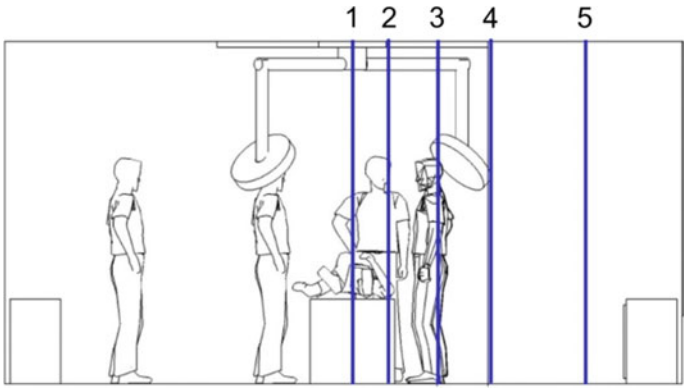

Fig. 3.16 CFD grid refinement measurement locations in central cross-sectional plane (1. center of room; 2. interior edge of diffuser; 3. midpoint of diffuser; 4. exterior edge of diffuser; 5. midpoint of outer region of room)

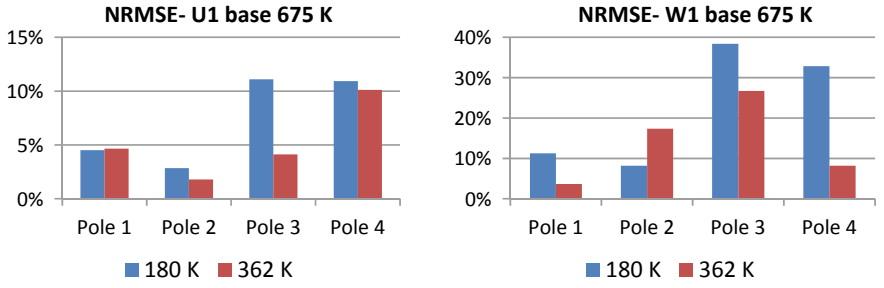

Fig. 3.17 NRMSE comparison between 180 and 362 K meshes and 675 K mesh

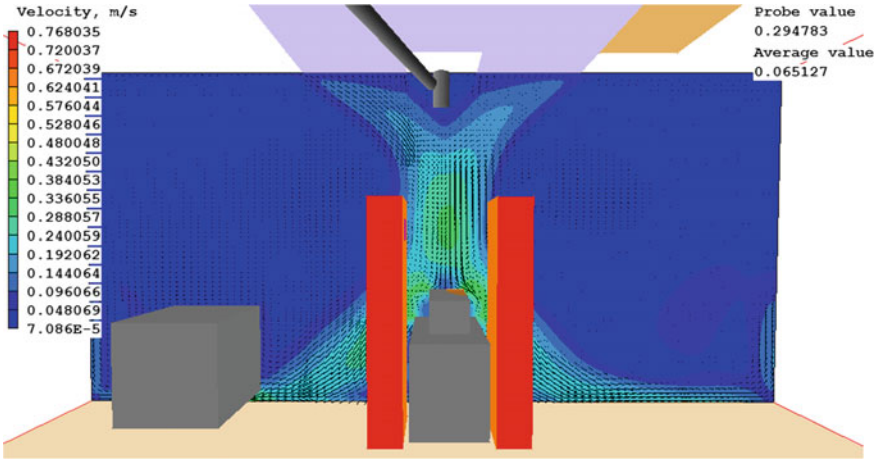

Fig. 3.18 Velocity vectors and contours at the central cross section with 675 K grid

The quantitative comparisons of simulation and experimental results were plotted in Figs. 3.19 and 3.20, for U (X) and W (Z) velocity component, respectively. Figures 3.19 and 3.20 show that the CFD simulations closely follow the experimental results, with a few exceptions (e.g., right above the patient body at Pole 1). It also appears that there is, in general, a large difference between the experimental results and the 180 K mesh, but a smaller difference between the 362 and 675 K meshes.

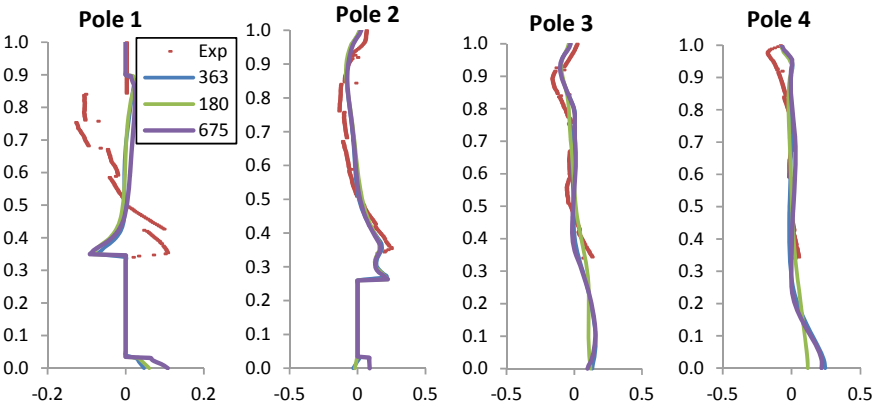

Fig. 3.19 Comparison of U-velocity in X direction

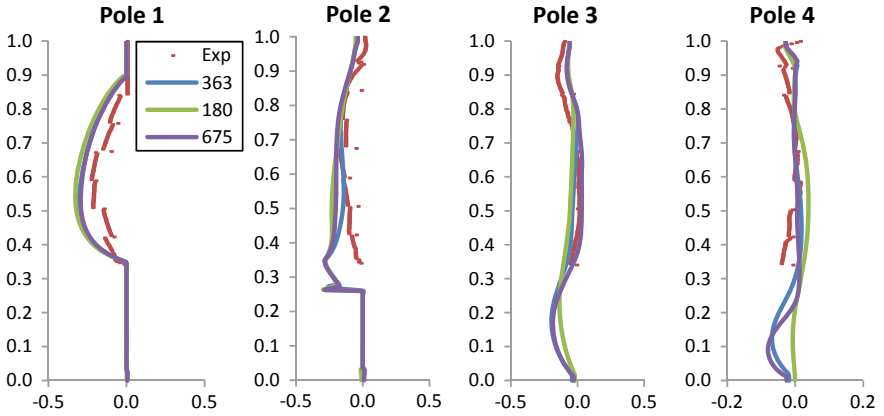

Fig. 3.20 Comparison of W-velocity in Z direction

(c) **Discussion of Results**

This example was used to demonstrate the applicability of using CFD for modeling and analysis of the surgical environment air flow. While CFD can be accurately used for modeling indoor air distribution in operating rooms, CFD user must be extremely careful in implementing these models to insure accurate simulation of air flow. The sensitivity of air flow to thermal characteristics of the indoor environment makes the model sensitive to heat gain input parameters. The heat gain and inlet boundary conditions must be carefully selected to ensure that the resulting air distribution patterns are correct.

The general indoor environment conditions place the operating room indoor air distribution in the mixed convection regime, but high cooling loads can lead to a strongly buoyancy-driven flow that is verified by the parametric study of the Archimedes number of supply air jet in the OR. The study reveals that the dependence of the room air distribution on the Archimedes number of supply air jet, instead of face velocity of supply diffuser, is of significant importance.

Assignment-3: Simulating Wind Flow Pattern across an Urban Environment

Objectives:

This assignment will use a computational fluid dynamics (CFD) program to model the wind-driven airflow distribution over an urban environment.

Key learning point:

- Urban wind simulation with appropriate domain sizes
- Wind profile input.

Simulation Steps:

(1) Build a (few) block(s) of buildings to represent a realistic community site (You may use map tools such as Google Earth to find some info);

   a. For those of you familiar with SketchUp (free tool), you may also consider to download building block models from Google SketchUp 3D warehouse for some specific real location in the world;
   b. You need to convert the SketchUp model into a certain suitable format that can be recognized and imported into the CFD software. Cleaning work is needed most of time to correctly use SketchUp models in CFD tools.

(2) Select appropriate outdoor domain sizes to be modeled;
(3) Study local weather data and identify representative wind conditions (directions, speeds, changes, frequencies, etc.);
(4) Establish corresponding boundary conditions, particularly the wind profile [isothermal case only: no temperature];
(5) Select a turbulence model: the standard k-ε model;
(6) Define convergence criterion: 0.1%;
(7) Set iteration: at least 1000 steps for steady simulation;
(8) Determine proper grid resolution with local refinement: at least 400,000 cells.

Cases to Be Simulated:

(1) Steady flow of wind over the building complex.

Report:

(1) Case descriptions: description of the case
(2) Simulation details: computational domain, grid cells, convergence status

   - Figure of the grid used (on X-Z, X-Y planes);
   - Figure of simulation convergence records.

(3) Result and analysis

   - Figure of airflow vectors at the middle plane of the buildings;
   - Figure of pressure contours at the middle plane of the buildings;
   - Figure of velocity contours at the middle plane of the buildings.

(4) Conclusions (findings, result implications, CFD experience and lessons, etc.).

References

ASHRAE (2008) ANSI/ASHRAE Standard 170-2008. Ventilation of healthcare facilities. American Society of Heating, Refrigerating, and Air-Conditioning Engineers, Inc., Atlanta

Chen Q, Srebric J (2002) A procedure for verification, validation, and reporting of indoor environment CFD analyses. HVAC&R Res 8(2):201–216

Clift R, Gauvin WH (1970) The motion of particles in turbulent gas streams. In: Proceedings of Chemeca'70, vol 1, p 14

Cook G, Int-Hout D (2009) Air motion control in the hospital operating room. ASHRAE Trans 51(3):30–36

Crowe C, Sommerfeld M, Tsuji Y (1998) Multiphase flows with droplets and particles. CRC Press, Boca Raton

Jiang Y (2002) Study of natural ventilation in buildings with large eddy simulation. Ph.D. dissertation, Massachusetts Institute of Technology, Cambridge, MA, USA

Liu X, Zhai Z (2007) Identification of appropriate CFD models for simulating aerosol particle and droplet indoor transport. Indoor Built Environ 16(4):322–330 (SAGE)

Ludwig JC, Fueyo N, Malin MR (2004) The GENTRA user guide. CHAM Co

Melikov AK, Kaczmarczyk J (2007) Influence of geometry of thermal manikins on concentration distribution and personal exposure. Indoor Air 17(1):50–59

Srebric J, Chen Q (2002) Simplified numerical models for complex air supply diffusers. HVAC & R Res 8:277–294

Wang H, Zhai Z (2012) Analyzing grid-independency and numerical viscosity of computational fluid dynamics for indoor environment applications. Build Environ 52:107–118

Yakhot V, Orszag SA (1986) Renormalization group analysis of turbulence. I. Basic theory. J Sci Comput 1:3–51

Zhai Z, McNeill J, Hertzberg J (2013) Experimental investigation of hospital operating room (OR) air distribution (TRP-1397). Final report to American Society of Heating, Refrigerating, and Air Conditioning Engineers, Inc., Atlanta, 158 p

Zhai Z, Osborne A (2013) Simulation-based feasibility study of improved air conditioning systems for hospital operating room. Front Archit Res 2(4):468–475

Zhang Z, Zhang W, Zhai Z, Chen Q (2007) Evaluation of various turbulence models in predicting airflow and turbulence in enclosed environments by CFD: Part-2: comparison with experimental data from literature. HVAC&R Res 13(6):871–886